Computers and Concrete, *Vol. 24, No. 3 (2019) 249-258*
DOI: https://doi.org/10.12989/cac.2019.24.3.249

Recovery of mortar-aggregate interface of fire-damaged concrete after post-fire curing

Lang Li[1,2a], Hong Zhang[2], Jiangfeng Dong[1], Hongen Zhang[1], Pu Jia[3], Qingyuan Wang[*1] and Yongjie Liu[**2]

[1]*Failure Mechanics & Engineering Disaster Prevention and Mitigation Key Laboratory of Sichuan Province, College of Architecture & Environment, Sichuan University, Chengdu 610065, China*
[2]*Key Laboratory of Deep Underground Science and Engineering, Ministry of Education, Sichuan University, Chengdu 610065, China*
[3]*Institute for Disaster Management & Reconstruction, Sichuan University, Chengdu, 610065, China*

(*Received February 28, 2019, Revised April 29, 2019, Accepted July 20, 2019*)

Abstract. In order to investigate the strength recovery of fire-damaged concrete after post-fire curing, concrete specimens were heating at 2°C/min or 5°C/min to 400, 600 and 800°C, and these exposed specimens were soaked in the water for 24 hours and following by 29-day post-fire curing. The compressive strength and split tensile strength of the high-temperature-exposed specimens before and after post-fire curing were tested. The proportion of split aggregate in the split surfaces was analyzed to evaluate the mortar-aggregate interfacial strength. After the post-fire curing process, the split tensile strength of specimens exposed to all temperatures was recovered significantly, while the recovery of compressive strength was only obvious within the specimens exposed to 600°C. The tensile strength is more sensitive to the mortar-aggregate interfacial cracks, which caused that the split tensile strength decreased more after high-temperature exposure and recovery more after post-fire curing than the compressive strength. The mortar-aggregate interfacial strength also showed remarkable recovery after post-fire curing, and it contributed to the recovery of split tensile strength.

Keywords: concrete; high temperature; post-fire curing; mortar-aggregate interface, image analysis

1. Introduction

Concrete, as the most widely used construction materials, may encounter elevated temperature like fire during serving (Kim and Kwak 2017). The mechanical properties of concrete decreased significantly after the exposure to over 400°C as a result of chemical and physical damages induced by elevated temperatures (Karataş *et al*. 2017, Ma *et al*. 2015). It was reported that the thermal-induced damages can be substantially recovered if the concrete was re-cured with enough water after the exposure to high temperatures. In the 1970s, Crook and Murray (1970) reported that the concrete can regain its strength if it was submerged in water after the high-temperature exposure. In 2001, Poon *et al*. (2001) reported that the compressive strength can be recovered to as much as 90% of the initial strength with 56 days of re-curing in water after the exposure to 600°C. In the following dozen years, some more studies about the autogenous recovery by post-fire curing have been reported (Henry *et al*. 2013, 2014, Li *et al*. 2017a, 2014, Lin *et al*. 2011, Park *et al*. 2015).

It was generally believed that the recovery is the result of the rehydration of the dehydrated phases produced during the high-temperature exposure, and the hydration of some unhydrated cement grains also contributes to the recovery (Poon *et al*. 2001). At high temperature, the hardened cement paste undergoes chemical changes. Ettringite starts to dehydrate over 60°C (Mantellato *et al*. 2016). The C-S-H chains begin to lose chemical bond water to shorter chains above 200°C (Piasta *et al*. 1984), and completely dehydrate to anhydrous phase at 750°C, but its structure was different from the unhydrated C_nS (Alonso and Fernandez 2004). At the temperature below 400°C, the unhydrated cement grains get further hydrated due to the internal autoclaving condition caused by the evaporation of water and high temperature (Khoury 1992, Sarshar and Khoury 1993, Wang *et al*. 2015). At about 450°C, the $Ca(OH)_2$ dehydrates quickly to CaO (Castellote *et al*. 2004, Zhang and Ye 2012). The dehydrated phases can get rehydrated in the post-fire curing process, and these rehydrated products can fill the thermal-induced cracks and pores to rebuild the microstructure of the cement matrix (Karahan 2011, Lin *et al*. 1996, Poon *et al*. 2001, Shui *et al*. 2008).

Crook and Murray (1970) believed that the CaO rehydrated to $Ca(OH)_2$ during post-fire curing, and then further carbonated to $CaCO_3$, which segmented the thermal-induced pores into smaller ones, consequently, the strength was recovered. Poon *et al*. (2001) found that the post-fire curing can reduce both the porosity and average pore size of thermal-damaged concrete, and it helped the strength and durability recovery. Shui *et al*. (2008) reported that the rehydrated C-S-H (hydrated calcium silicate) helped reconstruct the microstructures of the cement paste.

∗Corresponding author, Professor
E-mail: wangqy@scu.edu.cn
**Corresponding author, Associate Professor
E-mail: liuyongjie@scu.edu.cn
[a]Ph.D.
E-mail: li_lang@outlook.com

ISSN: 1598-8198 (Print), 1598-818X (Online)

With the help of X-ray CT (computed tomography), Henry *et al*. (2014) further found that the connectivity of the pores was decreased after post-fire curing.

Since the rehydration of the dehydrated phase is the base of the recovery by post-fire curing, Henry *et al*. (2011) pointed out that the interfacial cracks could just be partly healed because the rehydrated products formed only on one side of the cracks while those in the paste formed in both sides of the cracks. However, the strength of concrete is largely affected, even dominated by the interfacial strength, because the interfacial strength is lower than either the mortar or the aggregate. For the thermal-damaged concrete, the interfacial strength is more dominating because the interfaces of it were severely damaged due to the mismatched thermal expansion (Schneider 1988). Therefore, it is necessary to evaluate the changes of interfacial bond strength after elevated-temperature exposure and post-fire curing. After investigating the reports about the post-fire curing of thermal-damaged concrete, we found out that there were still no researches focused on the transformation of the interfacial bond strength. Therefore, we carried out this study to evaluate the evolution of the mortar-aggregate interfacial strength (it was abbreviated as interfacial strength in the following text, tables and figures) of concrete post-fire curing from 400, 600 and 800℃.

It is not easy to measure the interfacial strength directly, but it is possible to evaluate the interfacial strength indirectly by analyzing the split aggregate in the splitting surface of the concrete specimens. When splitting, the crack develops in two different paths in the zone of aggregate depending on the interfacial strength. If the interface is strong enough, the aggregate will be split, otherwise, the aggregate will be debonded from the mortar. Therefore, it is rational to evaluate the interfacial strength by analyzing the amount of split aggregate in the splitting surfaces. The computer-assisted image analysis has been introduced to the study of concrete (Felekoglu and Keskinates 2016, Hwang *et al*. 2010, Peng *et al*. 2012), and it makes it possible to analyze the splitting aggregate with the images of splitting surfaces. Elices and Rocco (2008) used the proportion of the split aggregate to classify the fracture type of specimen applied to three-point bending. With the same idea, Cülfik and Ö zturan (2010) used this method to detect the bond deteriorations of concrete exposed to high temperatures up to 250℃, with which the split aggregates on the splitting surfaces were analyzed after split tensile strength test.

For the concrete exposed to elevated temperature, the damage of the mortar-aggregate interface was directly responsible for the strength loss of concrete. And the damage generally aggravated with the increasing temperature (Ma *et al*. 2015). In another word, the proportion of the split aggregate would decrease with the increasing temperature if the aggregate strength remained unchanged, and it would increase if the mortar-aggregate interface was recovered. However, the studies on the recovery of the mortar-aggregate interface of fire-damaged concrete after post-fire curing were seldom reported. So, in this paper, the interfacial strength of concrete after fire exposure and post-fire curing was evaluated by analysis the split aggregate in the split surfaces, moreover, the change of the aggregate after high-temperature exposure was also taken in account. The object of this paper was to investigate the changes of the interfacial strength of concrete after elevated temperature exposure and post-fire curing, furthermore, to figure out how the interfacial strength recovery benefits the strength recovery of thermal-damaged concrete after post-fire curing.

Table 1 Mix proportion and strength of the concrete

Mix proportion (kg/m^3)							Compressive strength(MPa)	
cement	Fly ash	Sand	Coarse aggregate	S.P	Water	w/c ratio	28-day	90-day
412	103	571	1162	1.545	149	0.29	71.7	73.2

2. Experimental methodology

2.1 Materials and specimen preparation

Local ordinary 42.5R Portland cement in the brand of Esheng blended with 20 wt% low-calcium fly ash was used as the cementitious material. Local river sand was adopted as fine aggregate. Gravel between 4.75 and 20 mm with continuous size was used as coarse aggregates. For every cubic meter of fresh concrete, the dosage of cementitious material was 515 kg (made up with 103 kg of fly ash and 412 kg of cement); the fine aggregate was 571 kg; the coarse aggregate was 1162 kg; the water was 149 kg with the water to cementitious materials ratio of 0.29. Powdery polycarboxylic superplasticizer (S.P) at the weight ratio of 0.3% to the cementitious material was added to ensure the workability. The mix proportion of the concrete was shown in Table 1.

After well mixed in the blender, the fresh concrete was cast into the cubic molds with the edge length of 100 mm. Then the specimens within the molds were covered with a thin plastic film to keep the water from evaporating. The specimens were demolded in 24 hours after casting, then placed in the curing chamber at 20℃ with relative humidity (RH) of 95% until 28 days and followed by ambient curing up to 90 days. The compressive strength at 28 days and 90 days were shown in Table 1

2.2 High-temperature exposure and post-fire-curing

After curing for at least 90 days, the specimens were subjected to high-temperature exposure. The exposure was conducted with an electric furnace, in which the temperature can be controlled by the program precisely. As shown in Fig. 1, the specimens were heating at 2 or 5℃/min to the target temperatures, i.e., 400, 600 and 800℃, and maintained at the target temperature for 60 minutes before cooling in the furnace to the room temperatures. After cooling down to room temperature, specimens for post-fire curing were soaked in the water for 24 hours and then re-cured in the chamber at 20℃ with RH of 95% for another 29 days before the following tests. So, the whole post-fire curing process lasted for 30 days. While those did not need re-curing were subjected to the property

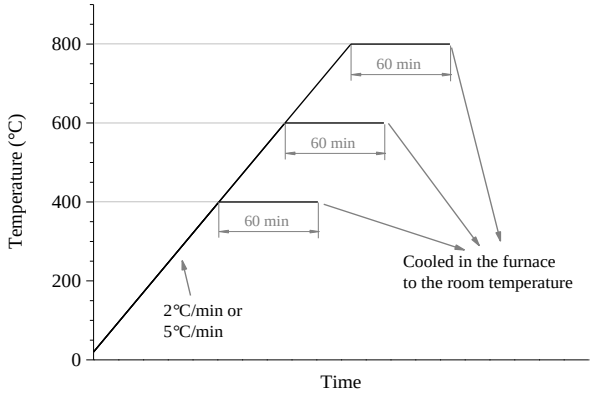

Fig. 1 Heating and cooling regimes

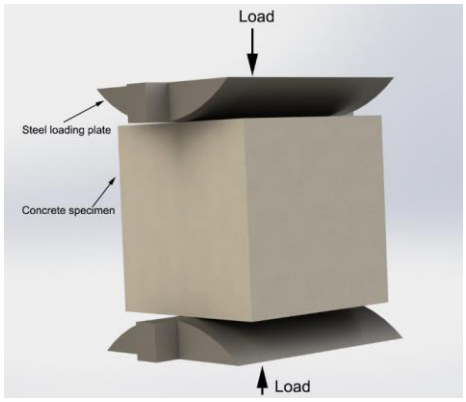

Fig. 2 Schematic splitting tensile strength testing method

tests within one day after cooling to avoid the further damages caused by the rehydration of CH.

2.3 Compressive strength

The compressive strength of those specimens was measured with the electrohydraulic servo-controlled compression test machine in Sichuan University, China. The loading capacity of this machine is 2000 kN, and the loading speed was 1 kN/s. For each group, the test was repeated twice to get an average compressive strength. In this study, 90-day compressive strength was used to refer to the compressive strength of unexposed specimens.

2.4 Splitting tensile strength

The splitting tensile strength was measured following the instruction of Chinese standard GB/T 50081-2002, the test method was shown in Fig. 2 schematically. The loading process was conducted on an electrohydraulic servo-controlled compression test machine with a loading capacity of 300 kN in Sichuan University, China. The loading rate was 0.5 kN/s. Like the compressive strength test, the splitting tensile strength test of each group was repeated twice to get the average value from three same specimens. With the ultimate load of the specimens, the splitting tensile strength can be calculated as

$$f_{ts} = \frac{2F}{\pi A} = 0.637\frac{F}{A} \quad (1)$$

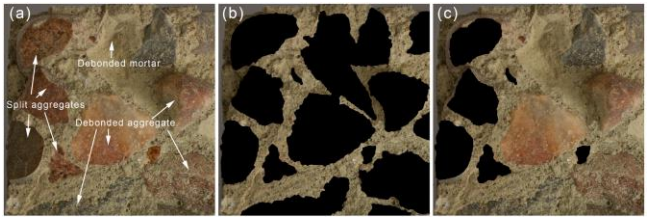

Fig. 3 Selection of the debonded mortar-aggregate interfaces: (a) the split surface; (b) selected all the aggregates and debonded interfaces; and (c) selected split aggregate

Where f_{ts} is the splitting tensile strength of the specimen, F is the ultimate load of the specimens, A is the area of the splitting surface, which is 1×10^4 mm^2 in this study.

2.5 Image analysis

After the splitting tensile strength test, the image of the split surfaces of each specimen was taken with a Nikon D90 digital single-lens reflex camera. Then the images were opened with Photoshop to select and color the area of split aggregates and those debonded ones in two different layers. It is worth noting that herein the term aggregate referred to the coarse aggregate if no specific introduction was given. For easy recognition in the next analyzing step, the selected areas in the images were colored as dark (R=0, G=0, B=0). Then the area of the split and debonded aggregate was calculated with MATLAB. To be specific, the proportion of the split aggregate, which is the ratio of the split aggregate to all the aggregate area in the split surface was calculated to evaluate the interfacial strength.

Here, it is necessary to define the split aggregate and the debonded aggregate. When splitting, the aggregate would be either split into two parts, which is defined as split aggregate, or debonded with the mortar, which is defined as debonded aggregate. As shown in Fig. 3(a), it is very easy to find the differences between the split aggregate with the debonded one visually. The split aggregate is very clean and with a clear boundary, while the debonded one is a little dusty and the boundary with the mortar is not as clear as the split one.

After the split tensile test, the specimen was split into two parts, and there is a split surface in each part. The two parts from the same specimen were complementary. For the split aggregate, it could be found in each split part, while for the debonded aggregate, it could only be found in one split part, and the debonded mortar can be found in the other split part, as the debonded mortar shown in Fig. 3(a). Therefore, when selecting the debonded aggregate, not only the debonded aggregate was selected, but also the debonded mortar as shown in Fig. 3(b). The selected results are shown in Fig. 4.

2.6 The strength of the aggregate

The proportion of split aggregate in the split surface was also affected by the strength of the aggregate, which would change along with the exposed temperatures. So, it is necessary to take the change of aggregate strength into account. Since the aggregate used in this study was made up

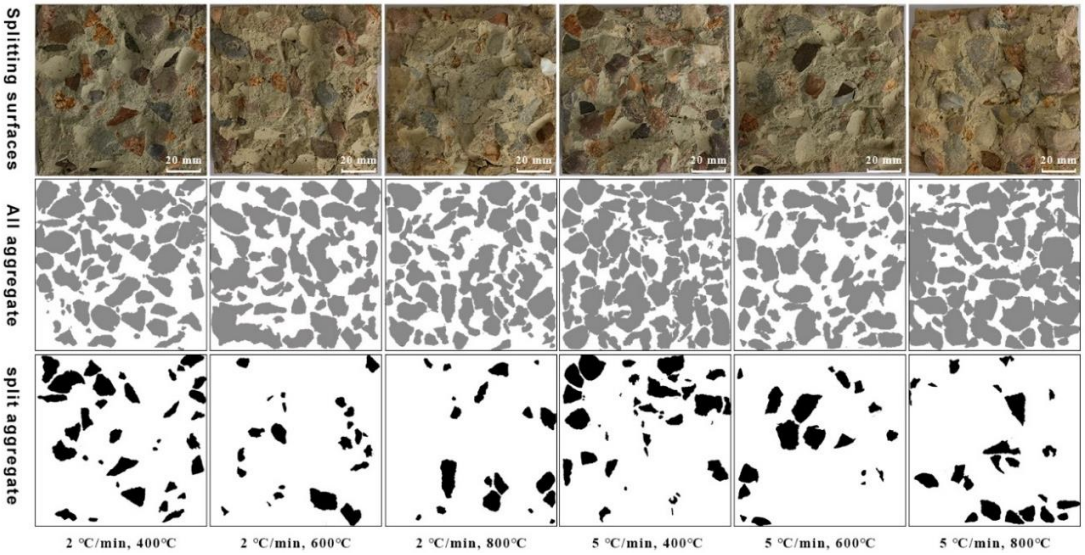

(a) Specimens after high-temperature exposure

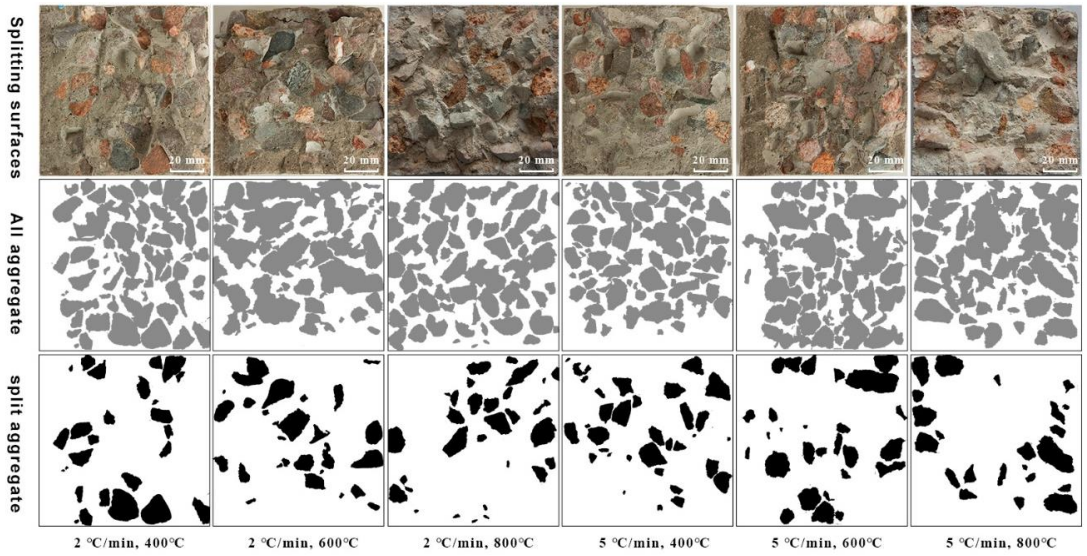

(b) Specimens after post-fire curing

Fig. 4 Selected results of all the aggregates and the split aggregates: (a) specimens after high-temperature exposure; and (b) specimens after post-fire curing

of several kinds of rock, it is not possible to measure the strength of the aggregate directly. Instead, we test the crush index of the aggregate following the instruction of Chinese standard GB/T 14685-2011, which is the standard of the pebble and crushed stone for construction. According to the standard, 3000 g of aggregate between 9.5 and 19 mm without any elongated or flat particle were sieved, and the sieved aggregate was filled in the device shown in Fig. 5. The device containing the aggregate was placed on the compression test machine with the maximum load of 300 kN at Sichuan University and loaded to 200 kN at the rate of 1 kN/s. The load of 200 kN was maintained for 5 seconds before unloading. Then the aggregate was moved out from the device and those passed the 2.36 mm sieve were weighed. The crush index of the aggregate was calculated as

$$Q_c = \frac{G_1 - G_2}{G_1} \times 100\% \quad (2)$$

Where Q_c is the crush index; G_1 is the mass of aggregate submitted to the test, which is 3000 g in this test; G_2 is the mass of aggregate pass the 2.36 mm sieve after the compression. For each group of aggregate, the test was repeated twice to get an average value.

To get the crush index of the aggregate after high-temperature exposure, the aggregate was subjected to the same exposure condition as the specimens. Also, a group of unexposed aggregate was also tested for comparison. As it was considered that the damages of the aggregate could not be recovered with post-fire curing (Henry *et al*. 2011), the crush index of the re-cured aggregate was not tested in this study.

3. Results and discussions

3.1 Compressive strength

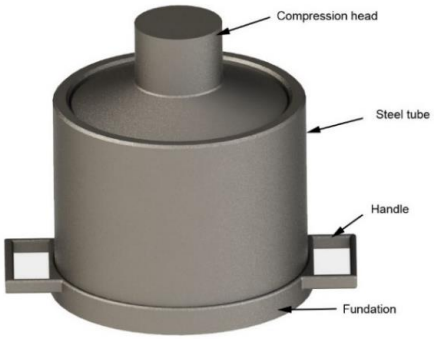

(a) 3-D model of the device

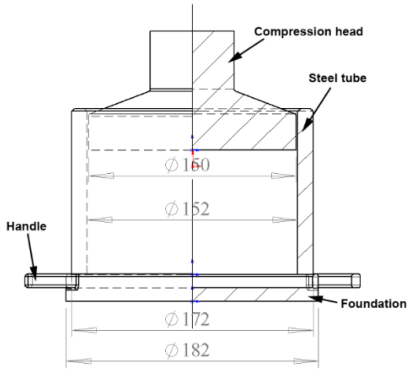

(b) Detailed size of the device

Fig. 5 Schematic of the device to test the crush index of the aggregate: (a) 3-D model of the device; and (b) detailed size of the device

Table 2 Compressive and split tensile strength of the specimens [a]

Exposed temperature	Heating rate	Compressive strength (MPa)			Split tensile strength (MPa)		
		unheated	heated	re-cured	unheated	heated	re-cured
400℃	2℃/min	73.2	59.2 (81)	60.2 (82)	3.38	1.87 (55)	2.36 (70)
	5℃/min		63.0 (86)	62.0 (85)		1.92 (57)	2.49 (74)
600℃	2℃/min		36.9 (50)	49.8 (68)		1.11 (33)	1.80 (53)
	5℃/min		39.5 (54)	48.9 (67)		1.19 (35)	1.82 (54)
800℃	2℃/min		21.0 (29)	21.1 (29)		0.83 (25)	1.05 (31)
	5℃/min		20.5 (28)	22.1 (30)		0.61 (18)	0.91 (27)

[a] Note: the values in the bracket is the relative strength.

The relative residual strength of specimens after exposure and recovered after re-curing is shown in Table 2 and Fig. 6. To present a more direct comparison, the relative strength was introduced, which was acquired by dividing the strength of the exposed or re-cured specimens by that of the unheated specimens, and it was present in percentage.

After the high-temperature exposure, the compressive strength of the specimens decreases obviously. The relative compressive strength of the specimens exposed to 400℃ heating at 2 and 5 ℃/min is 81% and 86%, respectively, and is 50% and 54% for those exposed to 600℃; after exposed to

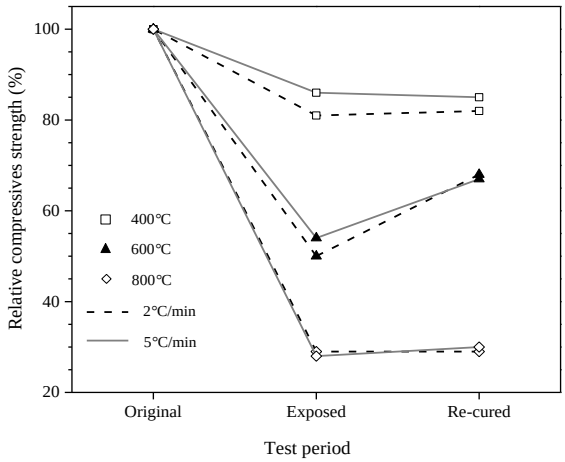

Fig. 6 Relative compressive strength of the specimens after the high-temperature exposure and post-fire curing

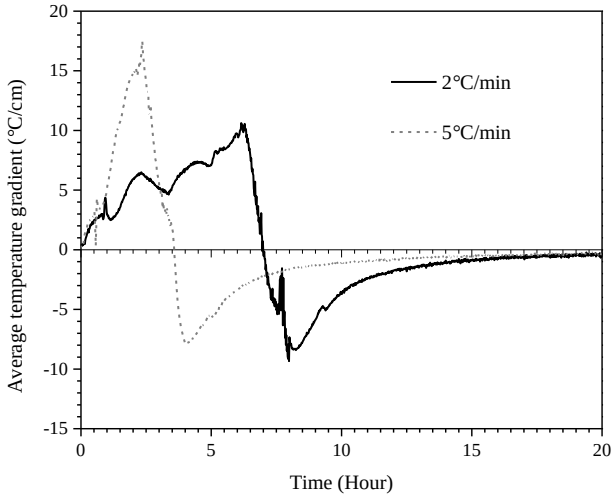

Fig. 7 Average temperature gradient between 2 and 5 cm to the surface of the specimens exposed to 800℃

800℃, it remains only 29% and 28%, respectively. Compared to the temperature, the heating rate shows relatively limited effects on the residual compressive strength, and its effect is getting more unobvious with the increasing temperature. After exposed to 400℃, the difference of the relative compressive strength between the two heating rates is 5 percentage points (pp), and it is 4 pp after exposed to 600℃, while it is only 1 pp when exposed to 800℃. The heating rate shows very limited effect because the temperature gradient it caused is limited. Schneider (1988) reported that the effect of heating rate is little as long as temperature gradients in the test specimens are lower than 10℃/cm. In this paper, we have measured the temperature history at the spots which were 2 and 5 cm to the specimen surface during the entire heating and cooling process with the method introduced in reference (Li *et al*. 2017a). And we have calculated the average temperature gradient between these two spots of the specimens exposed to 800℃, as shown in Fig. 7. The difference in the peak temperature gradient between these two heating rates is just about 8℃/cm, which is less than 10℃/cm, so the effects of the heating rate on the relative compressive strength is not obvious in this study.

Table 3 Highest temperature in the furnace and center of specimens with different heating rate (℃)

Target temperature	2℃/min		5℃/min	
	Furnace	Center of specimen	Furnace	Center of specimen
400℃	399	386	398	372
600℃	616	616	618	611
800℃	842	841	831	826

It is interesting that after exposure to 400℃ and 600℃, the specimens with a higher heating rate showed higher residual relative compressive strength. This phenomenon is familiar with our former study (Li *et al*. 2017a), in which the specimens cooled in the furnace with lower temperature gradient showed lower residual compressive strength compared to those cooled in the ambient environment with higher temperature gradient, because those cooled in the furnace reached higher temperature and consequently got severer damage. In this study, the peak temperature at the center of specimens were also measured, as shown in Table 3. Except for the 400℃, the temperature at the center of specimens heating at 2℃/min always reached the same level with the furnace while those heated at 5℃/min cannot. At the target temperature of 400℃, the specimens heating at 2℃/min reached 386℃ while those at 5℃/min only reached 372℃. And it is believed that the lower temperature at the center of the specimen is responsible for the 5 pp higher residual compressive strength of the specimens heating at 5℃/min.

After post-fire curing, the compressive strength recovered significantly for the specimens exposed to 600℃, while the recovery for those exposed to 400 and 800℃ were no more than 1 pp, as shown in Fig. 6. After exposed to 400℃, the number of rehydration products was not enough to make any effective recovery of the compressive strength. This temperature is not high enough for the CH to dehydrate to CaO (Zhang and Ye 2012), and the rehydrated C-S-H gels were separated without connecting to form the framework structure (Xuan and Shui 2011). Moreover, the hydration of the unhydrated cement also shows limited contribution to the recovery since its main product was a small quantity of CH (Hilloulin *et al*. 2016), which was thought to have little contribution to the compressive strength of concrete. Meanwhile, the rehydration of CaO to CH, which was accompanied with 95% of volume expansion, can cause further damages to the concrete because of the lack of thermal-induced cracks for the growth of CH (Henry *et al*. 2011, Wang *et al*. 2015). This is the reason why 1 pp decrease of compressive strength was observed in the specimens re-cured from 400℃ with the heating rate of 5℃/min. After exposed to 600℃, the CH was completely dehydrated to CaO, and a large amount of C-S-H has dehydrated to C_nS (Zhang and Ye 2012). These dehydrated products can quickly get rehydrated and heal the cracks, moreover, the rehydrated CH was believed to react to the fly ash to help the formation of C-S-H (Li *et al*. 2017a, Poon *et al*. 2001). Therefore, the compressive strength of concrete can be significantly recovered after post-fire curing. For the specimens re-curing from 800℃, although the lots of rehydration products were produced during post-fire curing, it was still hard to get a significant recovery on the compressive strength since the thermal-induced damage was too heavy.

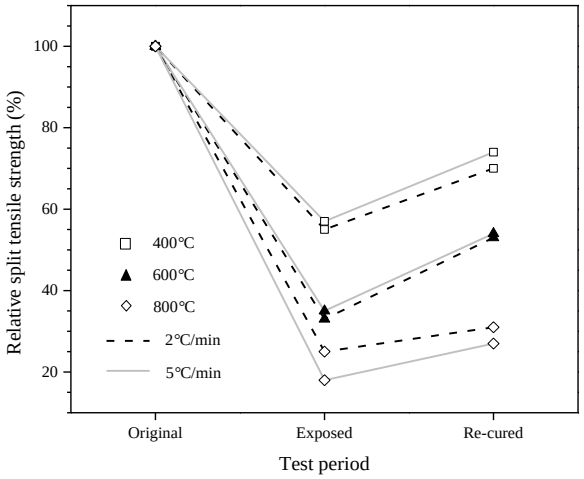

Fig. 8 Relative split tensile strength of specimens exposed to high temperatures and after post-fire curing

3.2 Splitting tensile strength

The split tensile strength of the specimens after the thermal exposure and post-fire curing were shown in Table 2. After exposed to 400℃, 45% and 43% of the split tensile strength were lost for the specimens heating at 2 and 5℃/min, respectively. And the strength loss increased with the increasing temperature. After 600℃, 67% and 65% of the split tensile strength were lost, and it only remained 25% and 18% of the split tensile strength after the exposure to 800℃. Comparing to the compressive strength, the tensile strength was much sensitive to the high temperature as it decreased more significantly after exposed to the same temperature. The result was accordant with that reported by Behnood and Ghandehari (2009). The differences between the compressive strength and split tensile strength can be explained by the different behavior of the thermal-induced cracks during different loading test. In splitting tensile test, the cracks decrease the load-carrying area and they tend to propagate and coalesce, while some of these cracks trends to close up under the compressive load during the compression test (Behnood and Ghandehari 2009, Cicekli *et al*. 2007).

Significant recovery of split tensile strength can be observed in specimens re-cured from all temperatures, as shown in Fig. 8, while that can only be observed in 600℃ for the compressive strength. After re-cured from 400℃, the split tensile strength recovered by 15 and 17 pp from 55% to 70% and 57% to 74% for the heating rate of 2 and 5℃/min, respectively, while the compressive strength showed no obvious recovery. The similar situation was observed in the specimens re-cured from 800℃. The split tensile strength recovered by 6 and 9 pp from 25% to 31% and 18% to 27%, respectively, while the recovery of compressive strength was no more than 2 pp. As we addressed before, this difference is because the split tensile

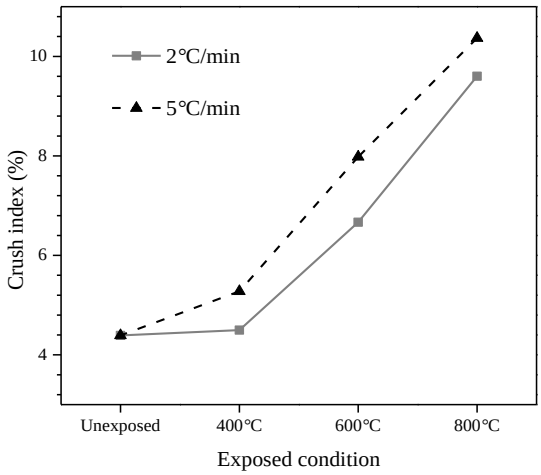

Fig. 9 Crush index of the aggregate after heating at different temperatures with different heating rates

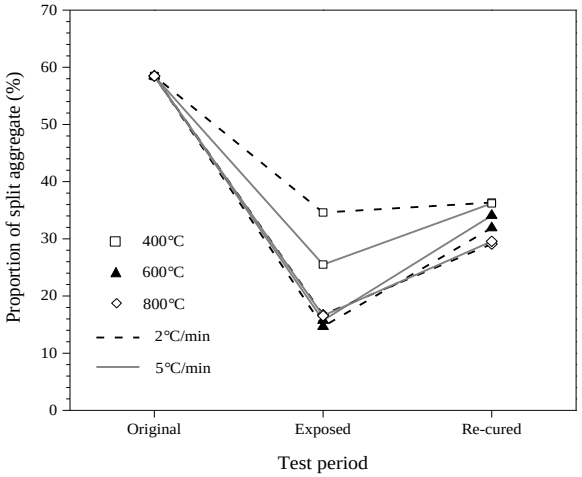

Fig. 10 Proportion of the split aggregate on the split surfaces of specimens exposed to high temperatures and post-fire curing

strength was much sensitive to the mortar-aggregate interfaces. Which means that the deterioration of the interface will cause more decrease in split tensile strength, and on the contrary, the recovery of the interface can be reflected more significantly by the split tensile strength. The best recovery of tensile strength in terms of recovered percentage points was also observed in the specimens re-cured from 600℃. At this temperature, the rehydration products were more than those exposed to 400℃, and the damage was not as server as those exposed to 800℃.

3.3 Crush index of the aggregate

As mentioned in section 2.6, the crush index was tested to evaluate the strength deterioration of the aggregate strength after high-temperature exposure. According to its definition, higher crush index means lower aggregate strength. The crush index of the aggregate exposed to different temperature was shown in Fig. 9. It is obvious that the aggregate exposed to higher temperature lost more strength, which means that higher temperature definitely causes severer damage to the aggregate (Liu and Xu 2015; Yang *et al*. 2017). With the same heating rate, the crush index increases almost linearly along with the temperature when the temperature exceeded 400℃. And at the same exposed temperature, the crush index of the aggregate heating at 5℃/min was higher than that at 2℃/min since the higher heating rate causes more damages to the aggregate (Li *et al*. 2017b; Wu *et al*. 2015). Especially for the temperature of 400℃, the aggregate heating at 2℃/min showed a very limited increase in crush index while that heating 5℃/min increase very significantly compared to the unheated aggregate.

3.4 Image analysis of split aggregate

As described in section 2.5, the proportion of the split aggregate was analyzed, and the results were shown in Fig. 10. The proportion of split aggregate is determined by both the aggregate strength and interfacial strength. Higher aggregate strength results in less split aggregate while higher interfacial strength results in more split aggregate. And, the proportion of split aggregate was a balanced result of these two factors.

For the unexposed specimen, the proportion of the split aggregate was 58.47%, and it decreased significantly after exposed to high temperatures because of the damages to the interfaces induced by the exposure. After exposed to 400℃, the proportion of split aggregate varies with the heating rate. It was 36.4% for the specimens heating at 2℃/min and 25.5% for 5℃/min. Meanwhile, after exposed to 400℃, the strength of aggregate decreased. This indicates that after the high-temperature exposure, the damage to the mortar-aggregate interface is much severer than it to the aggregate. Compare to 2℃/min, the less split aggregate heated at 5℃/min also indicates that the higher heating rate caused more loss of the interfacial strength at 400℃.

After exposed to 600℃ and 800℃, the proportion of split aggregate decreased to between 14% and 17%, which is a dozen percent point lower than 400℃. Considering the decrease of aggregate strength, the decrease of split aggregate indicates that the damage to the mortar-aggregate interface increase with the temperature. At the temperature of 600℃ and 800℃, the effect of heating rate on the proportion of split aggregate is not as significant as it at 400℃, as shown in Fig. 10.

At 600℃ and 800℃, the temperature has become the primary factor that causes damage to the interfaces rather than the heating rate. In this range of temperature, the thermal expansion of aggregate and cement paste are very different (Schneider 1988), and it can cause server damages to the interfaces by thermal-induced cracks (Fu *et al*. 2004a, c,b). Except for the heating rate, the effect of temperature on the proportion of split aggregate was also not obvious in this range of temperature. As shown in Fig. 10, the proportion of split aggregate of the specimens exposed to 600 and 800℃ are very similar. Its difference between 600℃ and 800℃ is much lower than that between 400℃ and 600℃. Moreover, the split aggregate of specimens exposed to 800℃ is slightly higher than those exposed to 600℃. It does not mean that the interfacial strength of

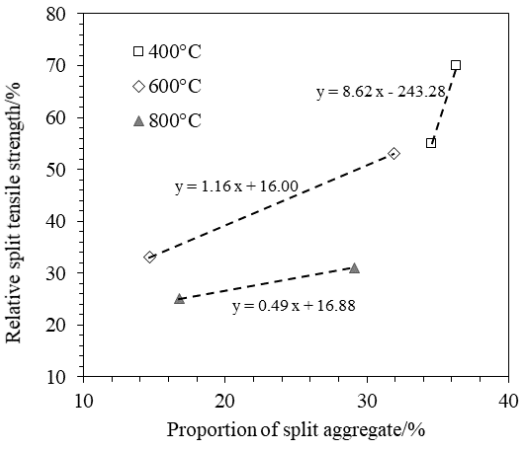

(a) 2℃/min

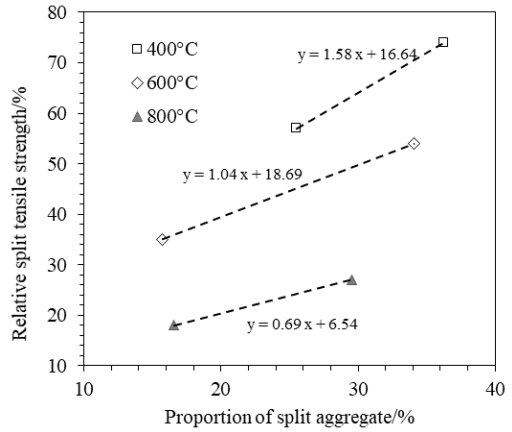

(b) 5℃/min

Fig. 11 Relationship between relative split tensile strength and proportion of split aggregate of specimens exposed at the rate of: (a) 2℃/min; and (b) 5℃/min

specimens exposed to 800℃ is stronger than those to 600℃. It indicates that at the exposed temperature of 800℃, the effect of aggregate strength on the proportion of split aggregate is more significant than that of the interfacial strength.

As shown in Fig. 10, the proportion of split aggregate of the re-cured specimens increased obviously, and it varies less with the temperature and heating rate compared to those just after the high-temperature exposure, falling in between 29% and 37%. It decreases with the increasing exposed temperature. It is 36.34% and 36.20% for those exposed to 400℃ at the heating rate of 2 and 5℃/min. For those re-cured from 600℃, the proportion of split aggregate is slightly lower, and it is 31.97% and 34.08% heating at 2 and 5℃/min. It is 29.09% and 29.57% for those re-cured from 800℃.

The increase of the split aggregate after post-fire curing indicates that the interfacial strength of fire-damaged concrete can be recovered by post-fire curing. It can be deduced from the proportion of split aggregate that after the post-fire curing, the interfacial strength of specimens decreased with the increasing exposed temperature. And the heating rate of 2 and 5℃/min shows very limited effect on the interfacial strength after the post-fire curing.

But in terms of the increase of the proportion of split aggregate after post-fire curing, which is the differences between that before and after the post-fire curing, the specimens exposed to 600℃ increased most obviously. It increases by about 17 to 18 pp for the heating rate of 2 and 5℃/min. Those re-cured from 800℃ increased by about 12 and 13 pp. For the specimens exposed to 400℃, it increases less than 2 pp for the heating rate of 2℃/min, while about 10 pp for those heating at 5℃/min.

As shown in Fig. 11, it is obvious that for the specimens exposed to the same temperature at the same heating rate, the split tensile strength of the specimens increased with the increasing proportion of split aggregate after the post-fire curing process. It indicates that for the specimens exposed to high temperatures, the recovery of the interfacial strength after post-fire curing is beneficial to the recovery of the split tensile strength. To link the two data points of the specimen before and after the post-fire curing with a straight line, the slope of the line can reflect the effect of interfacial strength on the split tensile strength. After the post-fire curing process, the strength of both the mortar and interface was recovered, and both can contribute to the recovery of the split tensile strength. Larger slope of the line in Fig. 11 means more contribute to the recovery of interfacial strength to the recovery of split tensile strength. For the same heating rate, the recovery of the interfacial strength of specimens exposed to lower temperature contributed more to the recovery of split tensile strength. Server damage of the interfacial strength was introduced by the higher temperature, and it was also harder to recovery after post-fire curing.

4. Conclusions

In this paper, concrete exposed at 400℃, 600℃ and 800℃ were re-cured for 30 days. The compressive strength and the split tensile strength were tested. Moreover, the proportion of split aggregate on the split surfaces was analyzed to evaluate the recovery of the interfacial strength after post-fire curing. Based on the experimental results, the main conclusions can be drawn as follow:

- With the post-fire curing method adopted in this paper, the compressive strength of concrete exposed at 600℃ can be recovered from about 50% to 68%, while those exposed at 800℃ can just be recovered by 2 pp to about 30%. So, it is worth applying post-fire curing to recovery the fire-damaged concrete exposed below 600℃.
- The recovery of split tensile strength was significant for all exposed temperatures, the recovery varied from 6 to 20 percentage points. After post-fire curing from 400℃ and 800℃, the recovery of split tensile strength was much more significant than the compressive strength because the split tensile strength was more sensitive to the mortar-aggregate interfacial cracks than the compressive strength.
- The increased proportion of split aggregate on the splitting surface after post-fire curing indicates the mortar-aggregate interfacial strength can be significantly recovered. The recovery of the interfacial strength

contributes to the recovery of split tensile strength, and the contribution is higher for the specimens exposed at lower temperature.

• At 600℃ and 800℃, the heating rate of 2℃/min and 5℃/min shows very limited effect on the compressive strength and split tensile strength. Because at these temperatures, the discordant thermal expansion between mortar and aggregate is the primary factor responsible for the damages.

Acknowledgments

The authors are sincerely grateful for the financial support provided by the National Natural Science Foundation of China (No. 11772209 & No. 11832007), the Basic scientific research fund for Central-Government-supported universities (Sichuan University), Postdoctoral fund of Sichuan University. The first author was supported by China Scholarship Council (CSC), which is sincerely appreciated.

References

Alonso, C. and Fernandez, L. (2004), "Dehydration and rehydration processes of cement paste exposed to high temperature environments", *J. Mater. Sci.*, **39**(9), 3015-3024. https://doi.org/10.1023/B:JMSC.0000025827.65956.18.

Behnood, A. and Ghandehari, M. (2009), "Comparison of compressive and splitting tensile strength of high-strength concrete with and without polypropylene fibers heated to high temperatures", *Fire Saf. J.*, **44**(8), 1015-1022. https://doi.org/10.1016/j.firesaf.2009.07.001.

Castellote, M., Alonso, C., Andrade, C., Turrillas, X. and Campo, J. (2004), "Composition and microstructural changes of cement pastes upon heating, as studied by neutron diffraction", *Cement Concrete Res.*, **34**(9), 1633-1644. https://doi.org/10.1016/S0008-8846(03)00229-1.

Cicekli, U., Voyiadjis, G.Z. and Abu Al-Rub, R.K. (2007), "A plasticity and anisotropic damage model for plain concrete", *Int. J. Plast.*, **23**(10-11), 1874-1900. https://doi.org/10.1016/j.ijplas.2007.03.006.

Crook, D.N. and Murray, M.J. (1970), "Regain of strength after firing of concrete", *Mag. Concrete Res.*, **22**(72), 149-154. https://doi.org/10.1680/macr.1970.22.72.149.

Cülfik, M.S. and Ö zturan, T. (2010), "Mechanical properties of normal and high strength concretes subjected to high temperatures and using image analysis to detect bond deteriorations", *Constr. Build. Mater.*, **24**(8), 1486-1493. https://doi.org/10.1016/j.conbuildmat.2010.01.020.

Elices, M. and Rocco, C.G. (2008), "Effect of aggregate size on the fracture and mechanical properties of a simple concrete", *Eng. Fract. Mech.*, **75**(13), 3839-3851. https://doi.org/10.1016/j.engfracmech.2008.02.011.

Felekoglu, B. and Keskinates, M. (2016), "Multiple cracking analysis of HTPP-ECC by digital image correlation method", *Comput. Concrete*, **17**(6), 831-848. https://doi.org/10.12989/cac.2016.17.6.831.

Fu, Y.F., Wong, Y.L., Poon, C.S., Tang, C.A. and Lin, P. (2004a), "Experimental study of micro/macro crack development and stress-strain relations of cement-based composite materials at elevated temperatures", *Cement Concrete Res.*, **34**(5), 789-797. https://doi.org/10.1016/j.cemconres.2003.08.029.

Fu, Y.F., Wong, Y.L., Tang, C.A. and Poon, C.S. (2004b), "Thermal induced stress and associated cracking in cement-based composite at elevated temperatures - Part I: Thermal cracking around single inclusion", *Cement Concrete Compos.*, **26**(2), 99-111. https://doi.org/10.1016/S0958-9465(03)00086-6.

Fu, Y.F., Wong, Y.L., Tang, C.A. and Poon, C.S. (2004c), "Thermal induced stress and associated cracking in cement-based composite at elevated temperatures - Part II: Thermal cracking around multiple inclusions", *Cement Concrete Compos.*, **26**(2), 113-126. https://doi.org/10.1016/S0958-9465(03)00087-8.

Henry, M., Darma, I.S., Haraguchi, Y. and Sugiyama, T. (2013), "Analysis of cracking in high-strength cementitious materials under heating and re-curing using X-ray CT", *Third International Conference on Sustainable Construction Materials and Technologies*, Tokyo, Japan.

Henry, M., Darma, I.S. and Sugiyama, T. (2014), "Analysis of the effect of heating and re-curing on the microstructure of high-strength concrete using X-ray CT", *Constr. Build. Mater.*, **67**, 37-46. https://doi.org/10.1016/j.conbuildmat.2013.11.007.

Henry, M., Suzuki, M. and Kato, Y. (2011), "Behavior of fire-damaged mortar under variable re-curing conditions", *ACI Mater. J.*, **108**(3), 281-289.

Hilloulin, B., Hilloulin, D., Grondin, F., Loukili, A. and De Belie, N. (2016), "Mechanical regains due to self-healing in cementitious materials: Experimental measurements and micro-mechanical model", *Cement Concrete Res.*, **80**, 21-32. https://doi.org/10.1016/j.cemconres.2015.11.005.

Hwang, C.L., Peng, S.S., Wang, E., Lin, S.H. and Huang, S.L. (2010), "A quantitative measurement of concrete air content using image analyses", *Comput. Concrete*, **7**(3), 239-247. https://doi.org/10.12989/cac.2010.7.3.239.

Karahan, O. (2011), "Residual compressive strength of fire-damaged mortar after post-fire-air-curing", *Fire Mater.*, **35**(8), 561-567. https://doi.org/10.1002/fam.1074.

Karataş, M., Balun, B. and Benli, A. (2017), "High temperature resistance of self-compacting lightweight mortar incorporating expanded perlite and pumice", *Comput. Concrete*, **19**(2), 121-126. https://doi.org/10.12989/cac.2017.19.2.121.

Khoury, G.A. (1992), "Compressive strength of concrete at high temperatures: a reassessment", *Mag. Concrete Res.*, **44**(161), 291-309. https://doi.org/10.1680/macr.1992.44.161.291.

Kim, G.J. and Kwak, H.G. (2017), "Depth-dependent evaluation of residual material properties of fire-damaged concrete", *Comput. Concrete*, **20**(4), 503-509. https://doi.org/10.12989/cac.2017.20.4.503.

Li, L., Jia, P., Dong, J., Shi, L., Zhang, G. and Wang, Q. (2017a), "Effects of cement dosage and cooling regimes on the compressive strength of concrete after post-fire-curing from 800℃", *Constr. Build. Mater.*, **142**, 208-220. https://doi.org/10.1016/j.conbuildmat.2017.03.053.

Li, M., Mao, X., Cao, L., Pu, H. and Lu, A. (2017b), "Influence of heating rate on the dynamic mechanical performance of coal measure rocks", *Int. J. Geomech.*, **17**(8), 04017020. https://doi.org/10.1061/(ASCE)GM.1943-5622.0000888.

Li, Q., Yuan, G. and Shu, Q. (2014), "Effects of heating/cooling on recovery of strength and carbonation resistance of fire-damaged concrete", *Mag. Concrete Res.*, **66**(18), 925-936. https://doi.org/10.1680/macr.14.00029.

Lin, W.M., Lin, T.D. and Powers-Couche, L.J. (1996), "Microstructures of fire-damaged concrete", *ACI Mater. J.*, **93**(3), 199-205.

Lin, Y., Hsiao, C., Yang, H. and Lin, Y.F. (2011), "The effect of post-fire-curing on strengthvelocity relationship for nondestructive assessment of fire-damaged concrete strength", *Fire Saf. J.*, **46**(4), 178-185.

https://doi.org/10.1016/j.firesaf.2011.01.006.
Liu, S. and Xu, J. (2015), "An experimental study on the physico-mechanical properties of two post-high-temperature rocks", *Eng. Geol.* **185**, 63-70. https://doi.org/10.1016/j.enggeo.2014.11.013.
Ma, Q., Guo, R., Zhao, Z., Lin, Z. and He, K. (2015), "Mechanical properties of concrete at high temperature-A review", *Constr. Build. Mater.*, **93**, 371-383. https://doi.org/10.1016/j.conbuildmat.2015.05.131.
Mantellato, S., Palacios, M. and Flatt, R.J. (2016), "Impact of sample preparation on the specific surface area of synthetic ettringite", *Cement Concrete Res.*, **86**, 20-28. https://doi.org/10.1016/j.cemconres.2016.04.005.
Park, S.J., Yim, H.J. and Kwak, H.G. (2015), "Effects of post-fire curing conditions on the restoration of material properties of fire-damaged concrete", *Constr. Build. Mater.*, **99**, 90-98. https://doi.org/10.1016/j.conbuildmat.2015.09.015.
Peng, S.S., Wang, E.H., Wang, H.Y. and Chou, Y.T. (2012), "Quality assessment of high performance concrete using digitized image elements", *Comput. Concrete*, **10**(4), 409-417. https://doi.org/10.12989/cac.2012.10.4.409.
Piasta, J., Sawicz, Z. and Rudzinski, L. (1984), "Changes in the structure of hardened cement paste due to high temperature", *Matériaux Constr.*, **17**(4), 291-296. https://doi.org/10.1007/BF02479085.
Poon, C.S., Azhar, S., Anson, M. and Wong, Y.L. (2001), "Strength and durability recovery of fire-damaged concrete after post-fire-curing", *Cement Concrete Res.*, **31**(9), 1307-1318. https://doi.org/10.1016/S0008-8846(01)00582-8.
Sarshar, R. and Khoury, G.A. (1993), "Material and environmental factors influencing the compressive strength of unsealed cement paste and concrete at high temperatures", *Mag. Concrete Res.*, **45**(162), 51-61. https://doi.org/10.1680/macr.1993.45.162.51.
Schneider, U. (1988), "Concrete at high temperatures - A general review", *Fire Saf. J.*, **13**(1), 55-68. https://doi.org/10.1016/0379-7112(88)90033-1.
Shui, Z., Xuan, D., Wan, H. and Cao, B. (2008), "Rehydration reactivity of recycled mortar from concrete waste experienced to thermal treatment", *Constr. Build. Mater.*, **22**(8), 1723-1729. https://doi.org/10.1016/j.conbuildmat.2007.05.012.
Wang, G., Zhang, C., Zhang, B., Li, Q. and Shui, Z. (2015), "Study on the high-temperature behavior and rehydration characteristics of hardened cement paste", *Fire Mater.*, **39**(8), 741-750. https://doi.org/10.1002/fam.2269.
Wu, D., Liu, G., Chen, S. and Sun, R. (2015), "An experimental investigation on heating rate effect in the thermal behavior of perhydrous bituminous coal during pyrolysis", *J. Therm. Anal. Calorim.*, **119**(3), 2195-2203. https://doi.org/10.1007/s10973-015-4401-y.
Xuan, D.X. and Shui, Z.H. (2011), "Rehydration activity of hydrated cement paste exposed to high temperature", *Fire Mater.*, **35**(7), 481-490. https://doi.org/10.1002/fam.1067.
Yang, S.Q., Ranjith, P.G., Jing, H.W., Tian, W.L. and Ju, Y. (2017), "An experimental investigation on thermal damage and failure mechanical behavior of granite after exposure to different high temperature treatments", *Geothermics*, **65**, 180-197. https://doi.org/10.1016/j.geothermics.2016.09.008.
Zhang, Q. and Ye, G. (2012), "Dehydration kinetics of Portland cement paste at high temperature", *J. Therm. Anal. Calorim.*, **110**(1), 153-158. https://doi.org/10.1007/s10973-012-2303-9.